Winter Storm Surge Event Long-Term Variability in the North Atlantic

Simon Barbot, Lucia Pineau-guillou, Jean-marc Delouis

JGR Oceans

RESEARCH ARTICLE
10.1029/2024JC022204

Winter Storm Surge Event Long-Term Variability in the North Atlantic

Simon Barbot[1,2], **Lucia Pineau-Guillou**[1], **and Jean-Marc Delouis**[1]

[1]Laboratoire d'Océanographie Physique et Spatiale, IUEM, Brest, France, [2]Université de Toulouse, LEGOS (CNES/CNRS/IRD/UT3), Toulouse, France

Key Points:

- Storm surge changes are investigated analyzing the fast-time and the slow-time components of surge events
- 74% of tide gauges in Europe and 45% in North America show major changes
- Last century changes show more linear trends in North America and more cyclical patterns in Europe

Supporting Information:

Supporting Information may be found in the online version of this article.

Correspondence to:

S. Barbot,
simon.barbot@univ-tlse3.fr

Citation:

Barbot, S., Pineau-Guillou, L., & Delouis, J.-M. (2025). Winter storm surge event long-term variability in the north Atlantic. *Journal of Geophysical Research: Oceans*, *130*, e2024JC022204. https://doi.org/10.1029/2024JC022204

Received 29 NOV 2024
Accepted 21 MAY 2025

Author Contributions:

Conceptualization: Simon Barbot, Lucia Pineau-Guillou
Data curation: Simon Barbot, Lucia Pineau-Guillou
Formal analysis: Simon Barbot
Funding acquisition: Lucia Pineau-Guillou
Investigation: Simon Barbot
Methodology: Simon Barbot, Lucia Pineau-Guillou, Jean-Marc Delouis
Project administration: Lucia Pineau-Guillou
Software: Simon Barbot, Lucia Pineau-Guillou
Supervision: Lucia Pineau-Guillou, Jean-Marc Delouis
Validation: Simon Barbot, Lucia Pineau-Guillou, Jean-Marc Delouis
Visualization: Simon Barbot
Writing – original draft: Simon Barbot

Abstract Changes in storm surge events are investigated using the Event CHARacterization method, which identifies and quantifies the various dynamical structures of a typical storm surge event. This method was applied yearly, using a 20 year sliding window, to a set of 41 long-term tide gauges in the North Atlantic. Storm surge events were investigated on the basis of four key parameters: the amplitude and duration of two structures related to atmospheric pressure (Gaussian structure) and wind stress (Laplace structure). The analysis reveals large changes in 71% of the tide gauges, located in the eastern North Sea, the Baltic Sea, and in specific regions of North America. Changes are more important for the duration (±16%) of the events than for the amplitude (±7%). In Europe, the pressure-induced structure (Gaussian) is more affected by changes than the wind-stress-induced structure (Laplace). In addition, the changes in North America show patterns with significant linear trends that lacked discernible geographical coherence, while in Europe, the changes exhibit cyclic patterns with more obvious geographical coherence.

Plain Language Summary Storm surges are caused by extreme weather systems such as storms and are responsible for coastal flooding. Considering the full dynamics of the events from 20 days before to 20 days after each maximum, most of the changes in storm surge events follow different cycles of 40–60 years, whereas only a few follow a strict linear trend. The duration of the events changes more rapidly than the amplitude of the elevation. The changes observed are quite different between the two sides of the North Atlantic. First, in North America, the changes due to the wind are more important, while in Europe, the changes due to the atmospheric pressure are more important. Second, in Europe, the pattern of the changes mostly follows cycles of 40–60 years, whereas in North America, the pattern of the changes is more linear.

1. Introduction

Storm surge refers to the additional elevation of the sea level due to low atmospheric pressure and strong winds that occur during storms (Pugh & Woodworth, 2014) and may be responsible for coastal floods, causing human and material losses. In the context of global climate change, the evolution of atmospheric extreme conditions also affects the occurrence and intensity of storm surge events (Seneviratne et al., 2021).

The present study intends to deepen the changes in storm surge events due to extratropical cyclones, especially since numerous studies have already assessed the changes due to tropical cyclones (Szopa et al., 2021). Even if there is high confidence that high water levels will be more frequent in the future due to the increase in sea level, there is only low confidence in whether future climate will increase storm surge at mid- or high latitudes (Seneviratne et al., 2021). This is due to the important interannual and decadal variability of extratropical cyclones.

In the literature, storm surge changes are mostly investigated analyzing parameters such as the peak surge elevation (maximum elevation of the event) (e.g., Calafat et al., 2022; Marcos et al., 2009; Menéndez & Woodworth, 2010; Tadesse et al., 2022; Talke et al., 2014; Wahl & Chambers, 2015, 2016), the duration of an event (time above a threshold; Haigh et al., 2010), or its intensity (area above a threshold; Zhang et al., 2000; Haigh et al., 2010). However, these parameters do not fully describe the temporal dynamics of a storm surge event (±10–20 days before and after the peak surge), partly missing the opportunity to isolate the influence of atmospheric pressure that can precede and follow the storm for a long time, especially in the Baltic Sea.

The new approach of Pineau-Guillou et al. (2023) introducing the Event CHARacterization (ECHAR) method, and then Barbot et al. (2024), is to separate the storm surge events of the North Atlantic into two structures: a

Writing – review & editing: Simon Barbot, Lucia Pineau-Guillou, Jean-Marc Delouis

slow-time Gaussian (up to ±20 days to the peak surge) that refers to the impact of atmospheric pressure and a fast-time Laplace (±1–2 days to the peak surge) that refers mainly to the impact of wind stress and secondarily to atmospheric pressure. This approach is quite relevant, as it provides an easier interpretation of the storm surge changes by distinguishing distinct physical processes. The typical storm surge event is thus described by four key parameters: the amplitude and duration of these two structures.

The present study will thus investigate the evolution of the storm surge event's full temporal dynamics by looking at the evolution of the four key parameters of amplitude and duration of Gaussian and Laplace structures. First, we will refer to the tide gauges where the parameters are changing the most, using a changing index. Descriptions will be organized around groups of tide gauges that show cyclic patterns, patterns with linear trend, or other types of change. Then, the additional understanding raised by this method will be compared to the standard ones and the robustness of the interpretations with respect to the length of the time series.

2. Data

The data set and methods are similar to those used in the study of (Barbot et al., 2024): 41 tide gauge time series are selected in the North Atlantic from the GESLA 3.0 (Caldwell & Merrifield, 2015; Haigh et al., 2022; Woodworth et al., 2016). The tide gauges are selected because the hourly time series began before 1940 and have at least 80 years of measurements without too many missing years. This consideration is motivated by the long-term variability observed in the return water level of Portland and Atlantic City (Wahl & Chambers, 2016) and by the high correlation with the winter North Atlantic Oscillation index (NAO) on European coasts (Menéndez & Woodworth, 2010). As the 20 year averaged NAO index shows an inflection around 1960 (Pinto & Raible, 2012; Talke et al., 2014), a few decades before this date are needed to distinguish long-term trends from other variability with great confidence.

The surge time series are obtained from the sea level data by removing the tides and the mean sea level (MSL). A sensitivity test has been conducted to investigate the impact of using the MSL rather than the median sea level, resulting in a very minor impact on the amplitude of the storm surges (±1.6% on average). The tides are predicted for each year based on the harmonic analysis of the 10 years before and 10 years after this year with 75 constituents (Tidal Toolbox software, Allain, 2014). Then, the MSL is calculated and removed for each winter (from 1st October to 30th March).

To investigate the link between winter storm surges and NAO, the Hurrell station-based monthly NAO index (Schneider et al., 2013) is averaged over the months of October to March to match the selected period of our data. The NAO index is one of the dominant indexes that explain the variability of storm surge in the North Atlantic (e.g., Mawdsley & Haigh, 2016; Marcos & Woodworth, 2017).

3. Methods

3.1. Typical Storm Surge Events Characterization

Similar to the two previous studies, storm surge events are selected as the five maximum instantaneous surges per winter (from 1 October to 31 March), with an independence criterion of 72 hr between the peak surges (Barbot et al., 2024; Pineau-Guillou et al., 2023). The event is observed over 20 days before and after the selected peak surges. We chose this 40 day period because storm surge events mostly last less than 40 days in the North Atlantic, with the longest storm surge observed in the Baltic Sea.

To obtain the evolution of storm surge events, the ECHAR method is used over a 20-year rolling window (Figure 1c). The typical event for each year is computed by stacking the events and computing the expected value hourly. Then, the typical events are decomposed into four structures. The two major structures are the long-time Gaussian, which is due to the atmospheric pressure (subset G) and the last-time Laplace, which is primarily due to the wind stress and secondarily to the atmospheric pressure (subset L). The secondary structures are the high-frequency oscillations, which are due to tide-surge interactions or nonstationary tides (subset O) and the negative surge for North American coasts, which is due to changes in wind direction (subset N), that is, when the wind suddenly turns and blows from the land to the sea, pushing the waters away from the coasts (Barbot et al., 2024). The typical event of the year y is characterized using the combination of these four empirical models:

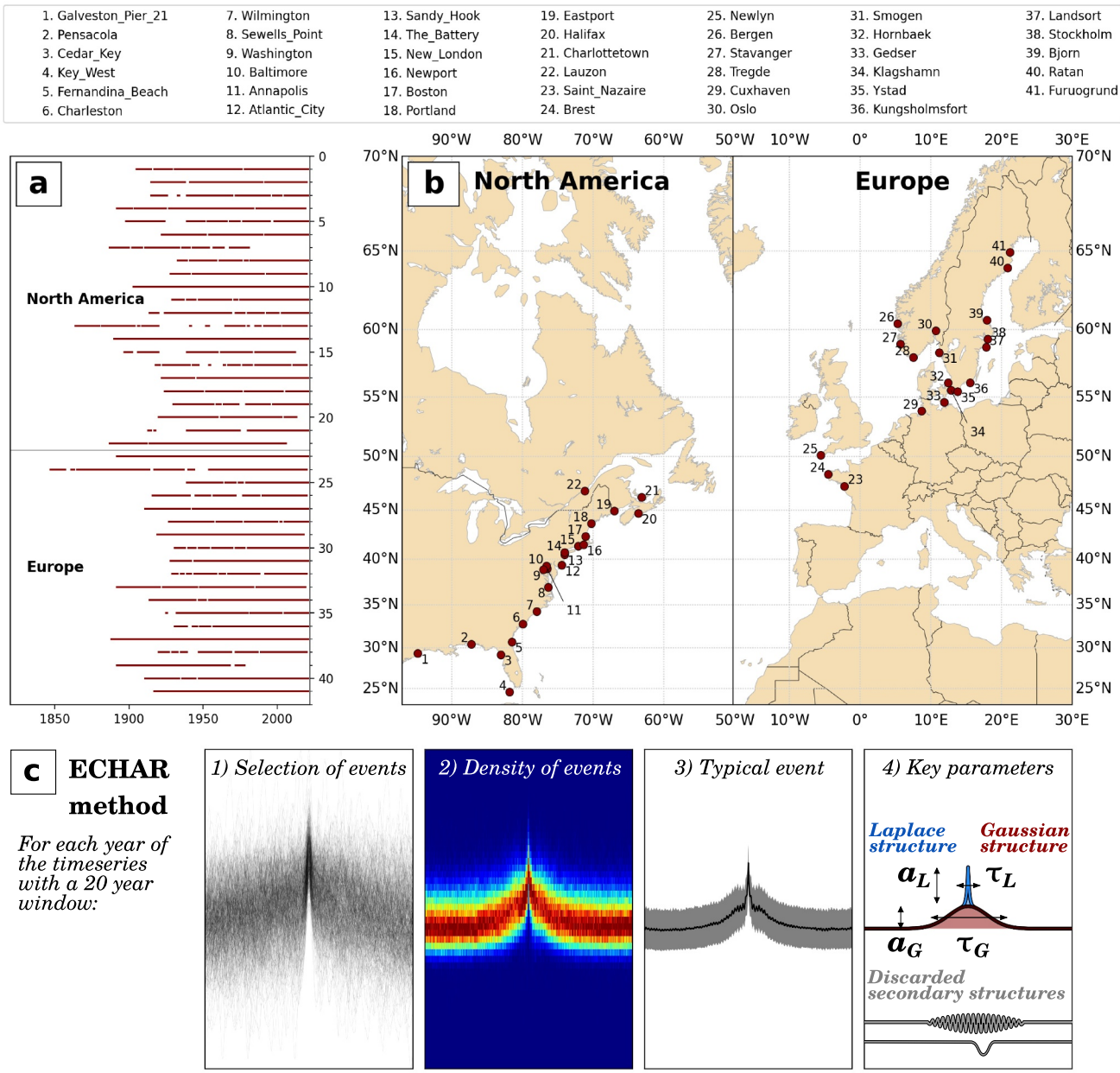

Figure 1. North Atlantic tide gauges used from GESLA 3.0 data set: (a) length, (b) location, and (c) synthesis of the methods to evaluate the evolution of the storm surge events through four key parameters. For (c) last panel (key parameters), note that the possible secondary structures (oscillations and negative surge) are estimated from the typical event and discarded for the rest of the study.

$$\eta_G^y(t) = a_G \exp\left(-\frac{1}{2}\left(\frac{t-\mu_G}{\sigma_G}\right)^2\right) \tag{1}$$

$$\eta_L^y(t) = \begin{cases} a_L \exp\left(-\sqrt{2}\ \frac{|t|}{\sigma_L}\right), & \text{if} \quad t > 0 \\ a_L \exp\left(-\sqrt{2}\ \frac{|t|}{k_L \sigma_L}\right), & \text{if} \quad t \le 0 \end{cases} \tag{2}$$

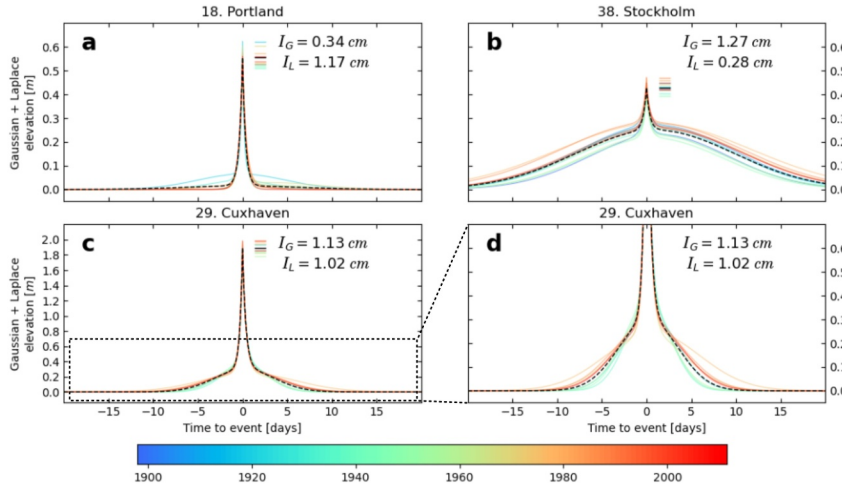

Figure 2. Evolution of the storm surge typical events (modeled with a Gaussian and Laplace structures) every 5 years at (a) Portland, (b) Stockholm, and (c) Cuxhaven. Note that Cuxhaven has been duplicated and zoomed in (d) in order to show a comparable scale with the two other tide gauges. The colored lines refer to the typical events along time and the black one refers to the reference typical event (calculated over the whole tide gauge period). The dashes next to the peak surge refer to the peak surge anomalies compared to the reference. Other tide gauges are available in Figures S2 and S3 in Supporting Information S1.

$$\eta_O^y(t) = a_O \cos\left(\omega_{M_2} t - \varphi_O\right) \exp\left(-\frac{1}{2}\left(\frac{t-\mu_O}{\sigma_O}\right)^2\right) \tag{3}$$

$$\eta_N^y(t) = a_N \exp\left(-\frac{1}{2}\left(\frac{t-\mu_N}{\sigma_N}\right)^2\right) \tag{4}$$

with η the sea level elevation, t the time to the peak surge, and ω_{M2} the tidal frequency for M2 harmonic constituent, the major one in the North Atlantic. The four key parameters of interest for this study are as follows: a_G, $\tau_G = 4\sigma_G$, a_L, and $\tau_L = 2\sigma_L(1 + k_L)$ (a for amplitude, τ for duration); and the secondary parameters are σ for standard deviation, μ for the delay to peak surge, k_L for the Laplace slope asymmetry, and φ_O for the phase of the oscillation.

Structure estimation is performed by finding the best fit of the model, restricted by ranges and prior values for the 13 parameters, and a weight that increases the importance of the fit around the peak surge (constraints available in Barbot et al., 2024). Once the four structures are estimated, only the major structure key parameters are kept for investigation: the Gaussian and Laplace amplitudes and durations (see Figure S1 in Supporting Information S1 for an example at Cuxhaven).

With the 20-year rolling window, yearly estimations of the four key parameters (a_G, τ_G, a_L, and τ_L) and associated Laplace and Gaussian structures ($\eta_G^y(t)$ and $\eta_L^y(t)$; Equations 1 and 2; colored lines in Figure 2) can be made. Note that a sensitivity study on the window size (using 10, 15, 25, or 30 years) attests to the similarity of the results and emphasizes that a 20-year window is a good compromise between smoother evolution (30 years) and more contrasted intensity (10 years).

3.2. Changing Index

In order to estimate which tide gauge is more subject to long-term changes, an index is proposed integrating the changes of the shape of the event (over 40 days, as an event is defined 20 days before and after the peak surge). First, for each structure X (Laplace or Gaussian) and each year y, the mean difference between the yearly shape η_X^y and the reference shape η_X^{ref} (the reference being calculated on the whole tide gauge period; black curve in Figure 2) is computed:

$$D_X(y) = \frac{1}{N_t} \sum_{t=-20}^{20} \left| \eta_X^y(t) - \eta_X^{ref}(t) \right| \quad (5)$$

with N_t the number of samples for the event (here one per hr for 40 days). This calculation is only performed where η_X^y and η_X^{ref} are not negligible (>1 mm) to have balanced indices between the two structures of different durations. Then, the changing index I is the standard deviation of this time series of mean difference:

$$I_X = \sqrt{\frac{1}{N_y}\left(\sum_y D_X(y) - \overline{D_X}\right)^2} \quad (6)$$

with N_y the number of defined years of the time series.

Using such a formula, I is expressed in meters, which is convenient to relate it to the elevation changes of the storm surge events. The downside of using a mean difference for D_X is that $D_X(y) = 0$ does not always ensure that $\eta_X^y(t)$ is not different from $\eta_{ref}(t)$ (cases where the upper differences match the lower differences). However, this case never occurs in the current study because the difference is made between two typical events with the same structures (Gaussian and Laplace).

As an illustration, the evolution of the shape of typical surge events and associated values of I_G and I_L are shown in Figure 2 for three tide gauges (other tide gauges available in Figures S2 and S3 in Supporting Information S1). Portland is selected for strong I_L (i.e., changes come mainly from the Laplace structure), Stockholm is selected for strong I_G (i.e., changes come mainly from the Gaussian structure), and Cuxhaven for both strong I_G and I_L. As the indexes I_G and I_L compute the hourly difference of the typical events, they take into account the variations of amplitude (Portland, Stockholm, and Cuxhaven) as well as the variations of duration (Cuxhaven). Moreover, the relative value between I_G and I_L helps to attribute the variability of the typical event to specific dynamics: to the Gaussian or Laplace part (as a reminder, the Gaussian structure is related to the atmospheric pressure before and after the storm, whereas the Laplace structure is primarily related to the wind stress and secondarily to the atmospheric pressure during the storm). For example, in Stockholm, the peak surge variability (represented by dashes in Figure 2b) can be attributed to a_G variability more than a_L variability (large I_G compared to small I_L), which suggests a variability of the atmospheric pressure fields more than surface winds. Further interpretations will be given in the next section.

3.3. Tide Gauge Clustering

In order to summarize the information, groups of tide gauges are proposed based on similar evolution for each of the four key parameters separately (i.e., the amplitude and duration of the Gaussian and Laplace structures). Our method is based on the site-by-site correlation matrix (Mawdsley & Haigh, 2016; Wahl & Chambers, 2015). First, the correlation matrix that compares the tide gauge parameters' evolution to each other is computed. Then, the values with $r < 0.7$ are set to zero in order to focus only on the tide gauges that have a highly correlated evolution. Finally, the clustering of the tide gauges based on this matrix is made using the complete linkage method (Manning et al., 2008), as this method greatly separates the tide gauges with low correlation. This method is repeated for the four key parameters. Because a high correlation does not imply a direct link to a common ocean dynamics, the groups obtained are only considered if they have geographic consistency.

3.4. Linear Trends and NAO Correlation

To compare our results to previous approaches in the literature (Calafat et al., 2022; Marcos & Woodworth, 2017; Menéndez & Woodworth, 2010; Wahl & Chambers, 2016; Woodworth et al., 2007), the linear trend and the NAO correlation are calculated for each tide gauge using the four key parameters of the Gaussian and Laplace structures (a_G, τ_G, a_L, τ_L) and the peak surge of the typical yearly storm surge event. The trends are calculated for the last century, from 1910 to 2010. For the time-averaged coherency with the storm surge ECHAR method, the winter NAO index is averaged over a 20-year window, then the correlation is made using the Pearson method (Pearson, 1895).

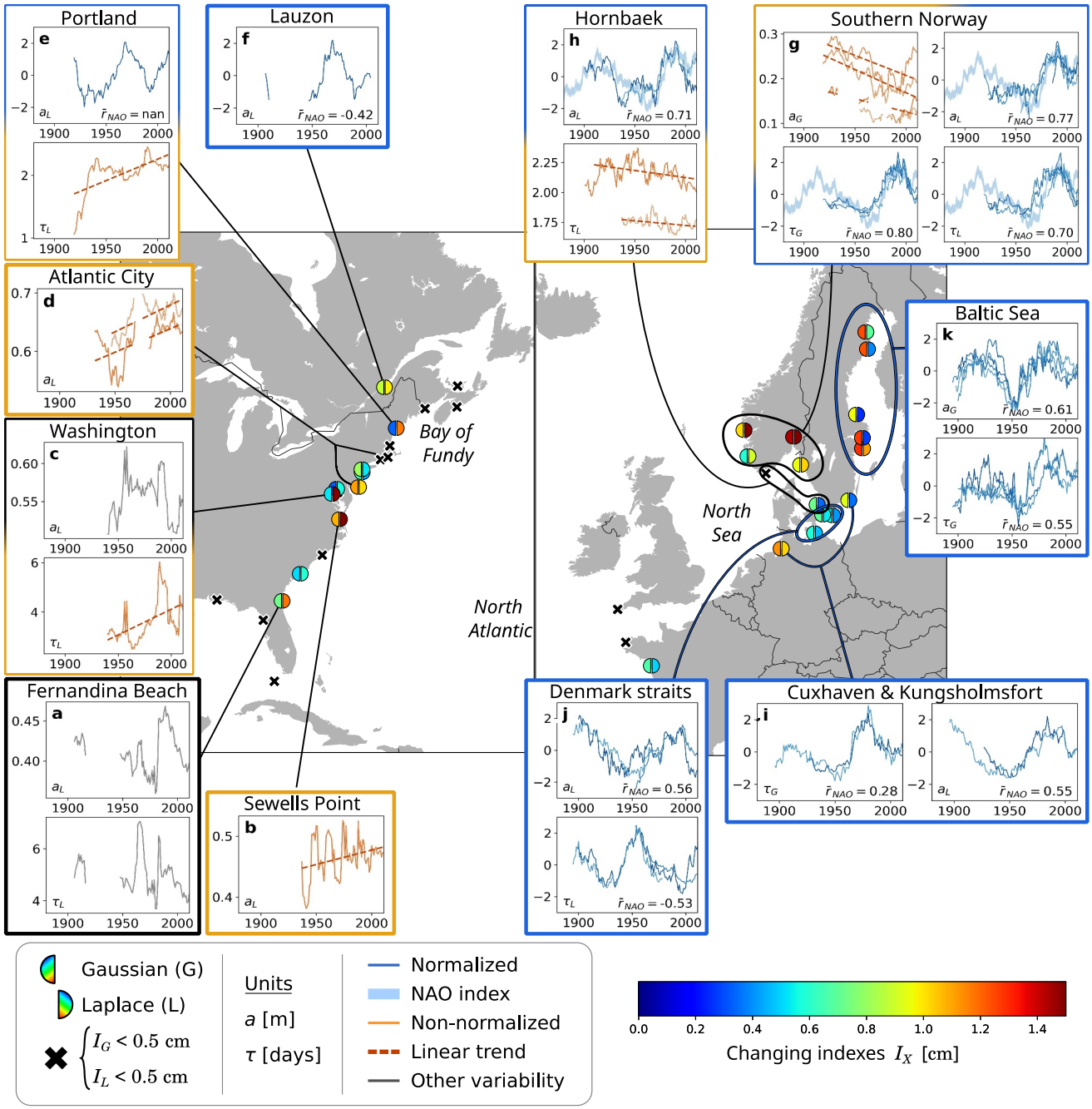

Figure 3. Changing indexes for Gaussian and Laplace structures. The evolution of the parameters (subplots a–k) are given for the tide gauges with $I_X > 0.5$ cm. Groups of tide gauges are made based on high intercorrelation coefficients for shown parameters. Blue subplots (e–k) indicate parameters with cyclic changes (in this case, amplitude and duration are normalized), whereas orange subplots (b–e, g, h) indicate changes with linear trends and black subplots (a, c) others changes (in this two last cases, amplitude and duration are not normalized, i.e., expressed in meters and days). In the blue subplots, the blue curves have been normalized to allow comparison with the NAO index (shaded blue curve when $\overline{r_{NAO}} > 0.7$).

4. Results

The investigation of the storm surge variability based on the complete shape of the storm surge event over numerous tide gauges results in a large number of evolution curves (four parameters over 41 tide gauges: 164 time series). Some choices have been made to select the most variable parameters and tide gauges. Figure 3 shows the changing indexes I_G and I_L on the background map and the groups with tide gauges showing $I_X > 0.5$ cm in the

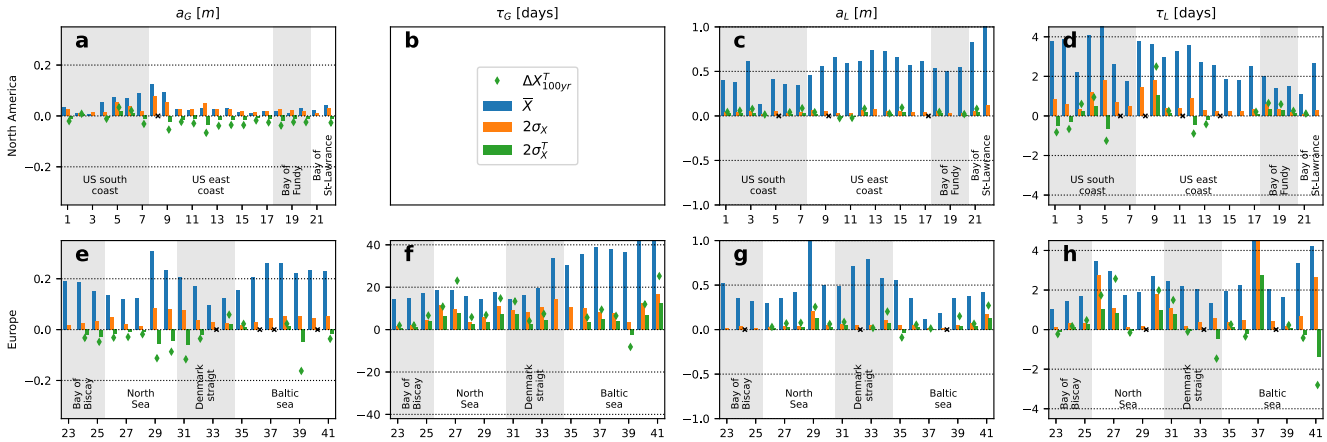

Figure 4. Variability over 1910–2010 period for each parameter (columns) in North America (a)–(d) and Europe (e)–(h) at each tide gauge. The blue bar refers to the mean value, the orange bar to the standard deviation, the green diamond refers to the evolution following a linear trend, and the green bar is the standard deviation of the linear trend. The values of τ_G in North America (b) have been hidden because these values are irrelevant due to the small amplitude of the Gaussian structure.

subplots (i.e., tide gauges where the parameters vary the most). This threshold leaves 76 time series to describe: 45 with temporal and spatial coherence shown and discussed in the present paper and 31 with noisy, singular, or incoherent patterns (not discussed here, see Figure S4 in Supporting Information S1). We first focus on the changing index values, then on the patterns of the evolution curves.

4.1. Changing Intensity

The use of the changing indexes I_G and I_L summarizes the extratropical storm surge event variability and helps us to set a variability threshold: if both indexes are < 0.5 cm, then the tide gauge is considered without major changes. Note that in North America, as the values of a_G are really small (Barbot et al., 2024), the variability of the Gaussian structure (I_G) is very minor for understanding typical storm surge events and will not be further described.

On the one hand, 41% of the tide gauges (17 of 41) do not show major changes (I_G and $I_L < 0.5$ cm, black crosses on the background map in Figure 3). In Europe, only 26% of the tide gauges are considered without major changes (5 out of 19), and they are mainly gathered along the Bay of Biscay and in the Danish Straits. In North America, 55% of the tide gauges are considered without significant changes (10 out of 22) and are distributed along the coasts without a clear pattern, suggesting very local causes of the changes.

On the other hand, 59% of the tide gauges (24 out of 41) display major changes (I_G or $I_L > 0.5$ cm). The geographic distribution of the changing index (background map of Figure 3) highlights hot regions such as the Baltic Sea ($0.9 < I_G < 1.4$ cm), southern Norway ($0.6 < I_L < 1.6$ cm) and Cuxhaven in the southeast of the North Sea ($I_G = 0.8$ and $I_L = 1.5$). The changes in storm surge events are mainly driven by the Laplace structure (i.e., wind effect) rather than the Gaussian structure (i.e., atmospheric pressure effect) everywhere except in the northern Baltic Sea. As described in Barbot et al. (2024), this area shows singular storm surge dynamics with $a_G \geqslant a_L$ because the surrounding lands reduce the wind speed, limiting the impact of wind stress during storm surges. Southern Norway and Cuxhaven are the only regions where strong variability is observed in both structures.

Now, the focus is on the tide gauges with major changes ($I_X > 0.5$ cm). To have an idea of how much the key parameters vary over time, the standard deviation is compared to the mean value for each parameter time series (Figure 4, orange and blue bars referring to the standard deviation and mean value). In North America, the standard deviation represents about 5% of the mean value for a_L and around 13% for τ_L. Thus, the duration τ_L is more variable than the amplitude a_L. In Europe, the standard deviation represents 11% of the mean value for a_G, 22% for τ_G, 7% for a_L, and 19% for τ_L. In this region, the duration is also more variable than the amplitude of both structures.

The parameters that show the strongest variability (still $I_X > 0.5$ cm) are described below according to three classes of long-term patterns. The first class refers to the cyclic changes (blue subplots in Figure 3), which occur

mostly on European coasts. These time series show a 40–60 year cycle with two modes since 1900. The second class refers to the changes that show significant trends without cyclic patterns (orange subplots), which occur mostly on American coasts. The third class refers to the other changes (black subplots), which will be discussed for two tide gauges on North American coasts.

4.2. Cyclic Changes

The time series are investigated by analyzing the observed cycles in the evolution of the parameters (blue subplots in Figure 3). The cycles observed in the North Sea, southern Norway, and the Baltic Sea are quite similar (blue subplots on Figures 3g–3i, and 3k). Such cycles are highly correlated with the winter NAO index for the tide gauges of southern Norway and Hornbaek ($\overline{r_{NAO}}$ of around 0.8 for a_L, τ_G, τ_L), but a weaker correlation is observed elsewhere $\left(0.29 < |\overline{r_{NAO}}| < 0.59\right)$. Note that the cycles observed in the Danish straits (Figure 3j) are rather anticorrelated to the winter NAO cycle $\left(\overline{r_{NAO}} = -0.55\right)$, whereas from both sides of the strait, the cycles are positively correlated. As shown by Barbot et al. (2024), the uncommon atmospheric pressure associated with the strongest storm surge and the narrowness of the Danish straits lead to a delay of the maximum of the Gaussian structure there. Such anticorrelated cycles of a_L and τ_L prove that specific ocean dynamics impact not only the Gaussian structure (associated with atmospheric pressure) but also the Laplace structure (associated with wind stress).

Two similar cycles are also observed on the North American coast for a_L in Portland and Lauzon (Figures 3e and 3f). Even if these cycles show quite similar frequency to NAO (approximately 50–60 years), the correlation with winter NAO is quite poor (respectively -0.2 and -0.5). Further discussion will be given in the next section.

4.3. Changes With Linear Trends

The time series are now investigated by analyzing the linear trend over the 1910–2010 period (orange subplots in Figure 3). In North America, among the 44 time series, 29 show significant trends, but only seven time series of a_L and two of τ_L show significant trends without any cyclic pattern. Similarly, along European coasts, among the 76 time series, 66 show significant trends, but only three time series of a_G, one of a_L, and six of τ_L show significant trends without clear cyclic variability. This means that, depending on the period used for trend estimation, significant trends will not be associated with long-term linear trends but will reflect a part of a longer cyclic change. For example, the time series of τ_G of southern Norway (Figure 3g) all show significant trends that explain 70% of the standard deviation, while these time series are also correlated with the winter NAO index of 0.85.

The time series of a_L at Galveston Pier and Sewells Point (orange subplots in Figures 3a and 3b) and of τ_L at Hornbaek (orange subplot in Figure 3h) respectively show significant positive and negative trends that have lasted since 1910. Such coherent long-term trends might certainly reflect a progressive change in storm surge dynamics. At Galveston Pier, Sewells Point, and Hornbaek, respectively, the standard deviation represents 5%, 7%, and 4% of the mean value, and the trend explains 84%, 30%, and 41% of it. However, in Washington, Atlantic City, and Portland (orange subplots in Figures 3c–3e), the trends might be significant, but they should still be taken with caution, as the time series are shorter than the others. Note that these trends could be different with a longer time series.

4.4. Other Changes

Finally, some tide gauges display major changes, though not cyclic and without significant linear trend. The time series of τ_L on the Galveston Pier (Figure 3a) and a_L on Washington (Figure 3c) show other patterns that seem quite coherent as long-term changes. The standard deviation represents 11% of the mean value at the Galveston Pier τ_L and 4% at Washington a_L.

5. Discussions

The results shown in this study focus on the evolution of the mean storm surges, considering the five highest events per winter. To address whether the changes highlighted here are relevant for other storm surge selection (e.g., one highest event per winter instead of five), the same analysis is performed for three different classes: first highest event per winter, second-third highest events per winter, and fourth-fifth events/winter (examples in Figure S5 in Supporting Information S1). Doing so is analogous to studying the percentile of the peak surges.

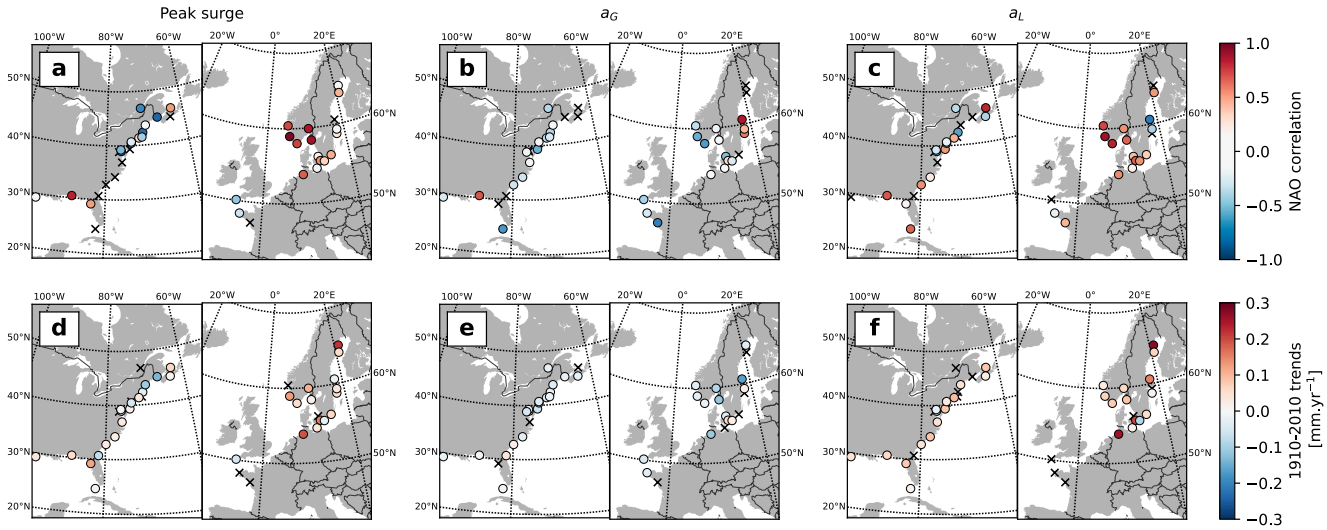

Figure 5. (a–c) NAO correlation and (d–f) linear trends for the yearly typical storm surge event in terms of (left) peak surge, (center) amplitude of the Gaussian structure and (right) amplitude of the Laplace structure.

Calculating the correlation between these new classes and the reference one (five highest events per winter), the evolution of the reference class ended up being similar (correlation > 0.6) to the other classes in 73% of the stations for a_L and 39% for τ_L. The key parameters of the Gaussian structure are only analyzed for Europe as the structure is not relevant in North America: 57% for a_G and 84% for τ_G have similar evolution no matter the class used. More similarities are observed in Europe than in North America (see Figure S6 in Supporting Information S1 for the maps). In conclusion, at most stations, the changes highlighted in the present study are relevant, even for more extreme events than those occurring five times per winter.

To compare our results with the existing literature, which generally focuses on standard metrics such as peak surge, the trends and correlations to the winter NAO index are computed for the three time series: peak surge, a_G, and a_L (Figure 5). The NAO index has been chosen because this index is one of the dominant indexes explaining the variability of storm surges in the North Atlantic (e.g., Mawdsley & Haigh, 2016; Marcos & Woodworth, 2017). Other indexes such as the Atlantic Multidecadal Oscillation (AMO) and Arctic Oscillation (AO) also capture similar variability and may explain minor additional variability. For example, in Portland (USA), Wahl and Chambers (2016) showed that combined NAO and AMO explained more variability (57%) than NAO alone (48%).

The positive correlation of NAO above 50°N and the negative correlation of NAO below observed with the peak surge (Figure 5a) match previous observations (e.g., Haigh et al., 2010; Menéndez & Woodworth, 2010; Talke et al., 2014; Marcos et al., 2015; Mawdsley & Haigh, 2016; Marcos & Woodworth, 2017) and can be mainly attributed to a_L (Figure 5c). However, the evolution of a_G in Europe is correlated with the NAO index for the Baltic Sea and anticorrelated elsewhere.

The positive trend of the peak surge observed in most tide gauges in the North American coasts (except in the Bay of Fundy; Figure 5d) is mostly due to the evolution a_L (Figure 5f). The negative trends in the Bay of Fundy are not explained by the two main structures and may be due to the evolution of the oscillation structure (not investigated here), since the oscillation amplitude is one of the strongest in this area due to the tidal resonance of the bay (Barbot et al., 2024). In the Baltic Sea, the peak surge trends are supported by both the Laplace and Gaussian structures, whereas the positive trends of the North Sea and southern Norway match the trend of the Laplace structure, despite the negative trend of the Gaussian structure.

However, the evolution curves shown in Figure 3 clearly show that linear models and correlation cannot fully capture the complexity of their shape. Zhang et al. (2000) and then Tadesse et al. (2022) highlight the dependency of the trends on the window used, which questions the significance of such metric in a context of high interannual and decadal variability. The p-value metric, often used to discriminate statistical significance, only states the relevance of the linear model (Greenland et al., 2016) and does not prevent discussion about the relevance of the

period. For example, Calafat et al. (2022) highlight significant trends over European coasts within the 1960–2018 period, but these trends, as they partially capture the internal variability, should not be extrapolated outside this window. Similarly, some of the trends observed in North America are based on shorter time series, so their relevance is less robust. Wahl and Chambers (2015) reported that with regard to storm surge sea level trends, 60–80 years of data are required to identify long-term trends "which are robust against the selected time period." For example, here, the time series of a_L in Atlantic City (Figure 3d), τ_L in Washington and Portland (Figures 3c–3e), and a_G in southern Norway (Figure 3g) show some inflection within the first or the last years. Thus, having a few additional years in the past or future could change the trend and our interpretation.

The exposed cyclic patterns (blue subplots in Figure 3) are only highly correlated with the winter NAO index in southern Norway, but less correlated elsewhere. The strong correlation in Norway is not surprising: the NAO has been designed to represent the atmospheric activity of the North Atlantic, and in this region, most of the storm tracks pass north of the British Islands and then reach Norway (Feser et al., 2021). Anderson (2002) and Dangendorf et al. (2014) show that the use of a more customized regional index, built with dedicated high- and low-pressure locations, increases the correlation with the 95th percentile of surge (Figure 5 in Dangendorf et al., 2014). Wahl and Chambers (2016) also highlight that the long-term cycle of the return water level at Portland was poorly explained by the winter NAO index but that a dedicated index could explain 87% of the variance (Figure 7 in Wahl & Chambers, 2016). This suggests that a similar long-term evolution pattern is taking place all over the North Atlantic but can be missed if the analysis is only supported by the NAO correlation coefficient. The spatial changes of this cyclic pattern can be a temporal shift that corresponds to the relative position of the tide gauges compared to the storm track: since the storm tracks are shifted in latitude with the evolution of the NAO index (Nie et al., 2008), the value of the NAO index that has the greatest impact on a tide gauge will not be the same for another tide gauge at a different location.

Finally, in North America, tide gauges without major changes (10 out of 22; black crosses in Figure 3) are distributed along the coasts without a clear pattern, suggesting very local causes of the changes. These local causes may be multiple. On the one hand, natural characteristics could be responsible for different local responses to a common evolving storm forcing. The shape of the coast or the bay where the tide gauge is located can act, in some cases, as a barrier to the propagation of the storm surge (Barbot et al., 2024): a narrow channel would limit the propagation of the storm surge in the bay (e.g., Fernandina Beach), the land aside long channels reduces the wind speed and limits the impact of the wind friction in storm surges (e.g., Stockholm with a weak Laplace structure). Thus, the evolution of the wind speed or the spatial range of the low pressure would result in different responses to such different contexts. On the other hand, the evolution of the geomorphology of the coasts (either from anthropic or natural causes) also controls how the tide gauges will be affected by the storm surges (De Leo et al., 2022; Familkhalili et al., 2020; Familkhalili & Talke, 2016; Talke & Jay, 2020).

6. Conclusion

The long-term variability of the storm surge event major shape is summarized by the evolution of four key parameters: the amplitude and duration of two structures, a slow-time Gaussian that refers to the atmospheric pressure impact and a fast-time Laplace that refers to the wind stress impact and secondarily to the atmospheric pressure. Focusing on the tide gauges that show a changing index $I_X > 0.5$ cm for at least one structure (71% of the tide gauges), the evolution curves of the parameters that present a coherent long-term pattern are described and the tide gauges that show similar changes are spatially grouped.

This threshold ($I_X > 0.5$) highlights that many tide gauges do not exhibit any major long-term changes or are weakly changing (small I_G and I_L) as in the Bay of Biscay and some dispersed tide gauges on the North American coasts. Not all key parameters are changing accordingly within each group, and some are too noisy to be relevant (parameters not shown in Figure 3).

Relative changes with respect to the mean are more important for the duration parameters (average standard deviation ±16%) than for the amplitude parameters (±7%). Based on the changing index, the Laplace structure (wind-related) dominates the changes in North America and the Gaussian structure (atmospheric pressure-related) dominates the changes in Europe. Both statistics point to more intense changes in Europe than in North America. The large cyclical patterns in Europe hide any linear trend, while clearer linear trends in North America can be observed. However, the shortness of some of the North American tide gauges alerts to relatively less robust conclusions. Therefore, we should be very careful with the usage of linear trend significance only, and future

studies would benefit from explicitly showing the curves more systematically to show the dynamics beyond the trends.

For future research, significant improvements can be made for the interpretation of the different cycles shown in European tide gauges by analyzing separately the storm tracks that affect southern, central, and northern Europe. Then, the calculation of dedicated indexes similar to the NAO index for each of the three storm configurations can be compared to cycles observed. The ECHAR method can be applied to additional regions after ensuring that the empirical model employed (Equations 1–4) aligns with the common events of these new regions. If different patterns are detected, then adjustments to the model should be taken into consideration.

Data Availability Statement

The GESLA data set of tide gauge measurements (Haigh et al., 2022) is available at https://gesla787883612.wordpress.com. The NAO index (Hurrell & Phillips, 2023) is available at https://climatedataguide.ucar.edu/climate-data/hurrell-north-atlantic-oscillation-nao-index-station-based. The Tidal Toolbox (Allain, 2014) can be installed by following https://sirocco.obs-mip.fr/other-tools/prepost-processing/comodo-tools/installation/.

Acknowledgments
This research has been supported by the French National Research Agency (ANR) Grant ClimEx (ANR-21-CE01-0004). We would like to thank the three anonymous reviewers who helped to strengthen this article with additional results (in supplement).

References

Allain, D. J. (2014). T-UGOm TidalToolbox. [Software] (Tech. Rep.). Retrieved from https://www5.obs-mip.fr/wp-content-omp/uploads/sites/12/2016/10/ttb-1.pdf

Anderson, H. C. (2002). Influence of long-term regional and large-scale atmospheric circulation on the baltic sea level. *Tellus A*, *54*(1), 76–88. https://doi.org/10.1034/j.1600-0870.2002.00288.x

Barbot, S., Pineau-Guillou, L., & Delouis, J.-M. (2024). Extreme storm surge events and associated dynamics in the north atlantic. *Journal of Geophysical Research: Oceans*, *129*(8), e2023JC020772. https://doi.org/10.1029/2023JC020772

Calafat, F. M., Wahl, T., Tadesse, M. G., & Sparrow, S. N. (2022). Trends in Europe storm surge extremes match the rate of sea-level rise. *Nature*, *603*(7903), 841–845. https://doi.org/10.1038/s41586-022-04426-5

Caldwell, P., & Merrifield, M. (2015). Joint archive for sea level. Data Report No. 24. *JIMAR Contribution No. 15-392*. Retrieved from http://ilikai.soest.hawaii.edu/UHSLC/jasl/datrep/JASL2015DataReport.pdf

Dangendorf, S., Müller-Navarra, S., Jensen, J., Schenk, F., Wahl, T., & Weisse, R. (2014). North sea storminess from a novel storm surge record since AD 1843*. *Journal of Climate*, *27*(10), 3582–3595. https://doi.org/10.1175/JCLI-D-13-00427.1

De Leo, F., Talke, S. A., Orton, P. M., & Wahl, T. (2022). The effect of harbor developments on future high-tide flooding in miami, Florida. *Journal of Geophysical Research: Oceans*, *127*(7), e2022JC018496. https://doi.org/10.1029/2022JC018496

Familkhalili, R., & Talke, S. A. (2016). The effect of channel deepening on tides and storm surge: A case study of wilmington. nc. *Geophysical Research Letters*, *43*(17), 9138–9147. https://doi.org/10.1002/2016GL069494

Familkhalili, R., Talke, S. A., & Jay, D. A. (2020). Tide-storm surge interactions in highly altered estuaries: How channel deepening increases surge vulnerability. *Journal of Geophysical Research: Oceans*, *125*(4), e2019JC015286. https://doi.org/10.1029/2019JC015286

Feser, F., Krueger, O., Woth, K., & van Garderen, L. (2021). North atlantic winter storm activity in modern reanalyses and pressure-based observations. *Journal of Climate*, *34*(7), 2411–2428. https://doi.org/10.1175/JCLI-D-20-0529.1

Greenland, S., Senn, S. J., Rothman, K. J., Carlin, J. B., Poole, C., Goodman, S. N., & Altman, D. G. (2016). Statistical tests, P values, confidence intervals, and power: A guide to misinterpretations. *European Journal of Epidemiology*, *31*(4), 337–350. https://doi.org/10.1007/s10654-016-0149-3

Haigh, I. D., Marcos, M., Talke, S. A., Woodworth, P. L., Hunter, J. R., Hague, B. S., et al. (2022). GESLA version 3: A major update to the global higher-frequency sea-level dataset. *Geoscience Data Journal*, *10*(3), 293–314. https://doi.org/10.1002/gdj3.174

Haigh, I. D., Nicholls, R., & Wells, N. (2010). Assessing changes in extreme sea levels: Application to the English Channel, 1900–2006. *Continental Shelf Research*, *30*(9), 1042–1055. https://doi.org/10.1016/j.csr.2010.02.002

Hurrell, J., & Phillips, A. (2023). The climate data guide: Hurrell North Atlantic Oscillation (NAO) index (station-based). [Dataset] (Tech. Rep.). Retrieved from https://climatedataguide.ucar.edu/climate-data/hurrell-north-atlantic-oscillation-nao-index-station-based

Manning, C. D., Raghavan, P., & Schütze, H. (2008). *Introduction to information retrieval*. Cambridge University Press. Retrieved from https://nlp.stanford.edu/IR-book/pdf/irbookonlinereading.pdf

Marcos, M., Calafat, F. M., Berihuete, Á., & Dangendorf, S. (2015). Long-term variations in global sea level extremes. *Journal of Geophysical Research: Oceans*, *120*(12), 8115–8134. https://doi.org/10.1002/2015JC011173

Marcos, M., Tsimplis, M. N., & Shaw, A. G. P. (2009). Sea level extremes in southern Europe. *Journal of Geophysical Research*, *114*(C1), 2008JC004912. https://doi.org/10.1029/2008JC004912

Marcos, M., & Woodworth, P. L. (2017). Spatiotemporal changes in extreme sea levels along the coasts of the North Atlantic and the Gulf of Mexico. *Journal of Geophysical Research: Oceans*, *122*(9), 7031–7048. https://doi.org/10.1002/2017JC013065

Mawdsley, R. J., & Haigh, I. D. (2016). Spatial and temporal variability and long-term trends in skew surges globally. *Frontiers in Marine Science*, *3*. https://doi.org/10.3389/fmars.2016.00029

Menéndez, M., & Woodworth, P. L. (2010). Changes in extreme high water levels based on a quasi-global tide-gauge data set. *Journal of Geophysical Research*, *115*(C10), 2009JC005997. https://doi.org/10.1029/2009JC005997

Nie, J., Wang, P., Yang, W., & Tan, B. (2008). Northern hemisphere storm tracks in strong AO anomaly winters. *Atmospheric Science Letters*, *9*(3), 153–159. https://doi.org/10.1002/asl.186

Pearson, K. (1895). Note on regression and inheritance in the case of two parents. *Proceedings of the Royal Society of London Series I*, *58*, 240–242.

Pineau-Guillou, L., Delouis, J., & Chapron, B. (2023). Characteristics of storm surge events along the North-East atlantic coasts. *Journal of Geophysical Research: Oceans*, *128*(4), e2022JC019493. https://doi.org/10.1029/2022JC019493

Pinto, J. G., & Raible, C. C. (2012). Past and recent changes in the north atlantic oscillation. *WIREs Climate Change*, *3*(1), 79–90. https://doi.org/10.1002/wcc.150

Pugh, D., & Woodworth, P. L. (2014). Sea-level science: Understanding tides, surges, tsunamis and mean Sea-level changes. (1st ed.). Cambridge University Press. https://doi.org/10.1017/CBO9781139235778

Schneider, D. P., Deser, C., Fasullo, J., & Trenberth, K. E. (2013). Climate data guide spurs discovery and understanding. *Eos, Transactions American Geophysical Union*, *94*(13), 121–122. https://doi.org/10.1002/2013EO130001

Seneviratne, S., Zhang, X., Adnan, M., Badi, W., Dereczynski, C., Di Luca, A., et al. (2021). Weather and climate extreme events in a changing climate [Book Section]. In V. Masson-Delmotte, et al. (Eds.), *Climate change 2021: The physical science basis. contribution of working group i to the sixth assessment report of the intergovernmental panel on climate change (chap. 11)*. https://doi.org/10.1017/9781009157896.013

Szopa, S., Naik, V., Adhikary, B., Artaxo, P., Berntsen, T., Collins, W., et al. (2021). Short-lived climate forcers [book section]. In V. Masson-Delmotte, et al. (Eds.), *Climate change 2021: The physical science basis. contribution of working group i to the sixth assessment report of the intergovernmental panel on climate change (chap. 6)*. https://doi.org/10.1017/9781009157896.008

Tadesse, M. G., Wahl, T., Rashid, M. M., Dangendorf, S., Rodríguez-Enríquez, A., & Talke, S. A. (2022). Long-term trends in storm surge climate derived from an ensemble of global surge reconstructions. *Scientific Reports*, *12*(1), 13307. https://doi.org/10.1038/s41598-022-17099-x

Talke, S. A., & Jay, D. A. (2020). Changing tides: The role of natural and anthropogenic factors. *Annual Review of Marine Science*, *12*(2020), 121–151. [Journal Article]. https://doi.org/10.1146/annurev-marine-010419-010727

Talke, S. A., Orton, P., & Jay, D. A. (2014). Increasing storm tides in New York Harbor, 1844-2013: INCREASING_stormtides_ny_1844to2013. *Geophysical Research Letters*, *41*(9), 3149–3155. https://doi.org/10.1002/2014GL059574

Wahl, T., & Chambers, D. P. (2015). Evidence for multidecadal variability in US extreme sea level records. *Journal of Geophysical Research: Oceans*, *120*(3), 1527–1544. https://doi.org/10.1002/2014JC010443

Wahl, T., & Chambers, D. P. (2016). Climate controls multidecadal variability in U. S. extreme sea level records. *Journal of Geophysical Research: Oceans*, *121*(2), 1274–1290. https://doi.org/10.1002/2015JC011057

Woodworth, P. L., Flather, R., Williams, J., Wakelin, S., & Jevrejeva, S. (2007). The dependence of UK extreme sea levels and storm surges on the North Atlantic Oscillation. *Continental Shelf Research*, *27*(7), 935–946. https://doi.org/10.1016/j.csr.2006.12.007

Woodworth, P. L., Hunter, J. R., Marcos, M., Caldwell, P., Menéndez, M., & Haigh, I. (2016). Towards a global higher-frequency sea level dataset. *Geoscience Data Journal*, *3*(2), 50–59. https://doi.org/10.1002/gdj3.42

Zhang, K., Douglas, B. C., & Leatherman, S. P. (2000). Twentieth-century storm activity along the U.S. East coast. *Journal of Climate*, *13*(10), 1748–1761. https://doi.org/10.1175/1520-0442(2000)013⟨1748:TCSAAT⟩2.0.CO;2